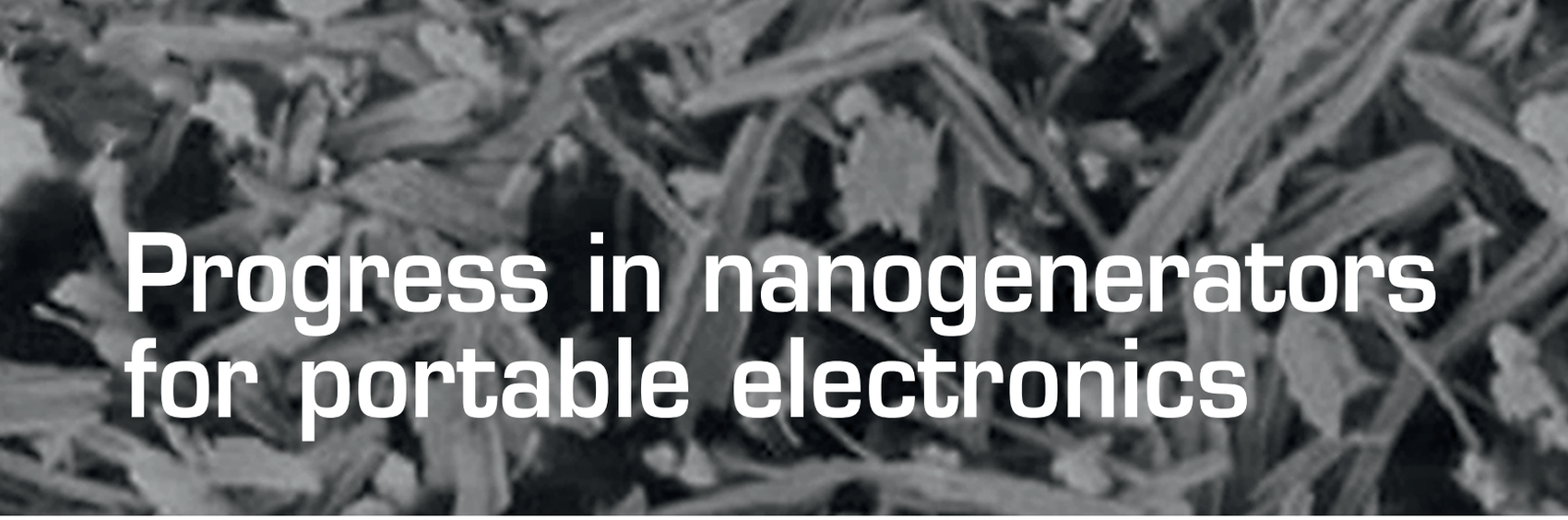

# Progress in nanogenerators for portable electronics

**Besides targeting at the worldwide energy needs at a large scope, we have been developing an area of nanoenergy, aiming at using nanotechnology to harvest the energy required for sustainable, independent and maintenance free operation of micro/nano-systems and mobile/portable electronics. As first reported in 2006, various nanogenerators (NGs) have been demonstrated using piezoelectric, triboelectric and pyroelectric effects. By using the energy from our living environment, our goal is to make self-powered system. The self-powering approaches developed here are a new paradigm in nanotechnology and green energy for truly achieving sustainable self-sufficient micro/nano-systems, which are of critical importance for sensing, medical science, infrastructure/environmental monitoring, defense technology and personal electronics.**

**Zhong Lin Wang*, Guang Zhu, Ya Yang, Sihong Wang, and Caofeng Pan**
*School of Materials Science and Engineering, Georgia Institute of Technology, Atlanta, USA*
**E-mail: zlwang@gatech.edu*

In the last half century, the developing trend of electronics has been miniaturization and portability. The history of computers is a typical example, from the vacuum tube based huge-size machines, to solid state MOSFET based main frame computers and later laptop computers, and now to handhold cell phones; the number of such computers the world possesses has changed from a few worldwide, to one per unit, and now one per person. The near future development concerns electronics that are much smaller than the size of a cell phone, so that on average each person can have dozens to hundreds small electronic systems. Such small size electronics and their working mode of operating like a sensor largely reduces power consumption, making it possible to use the energy harvested from our living environment to power it. It will become impractical if sensor networks have to be powered entirely by batteries because of the huge number of devices, large scale of distribution, and the difficulty of tracking and recycling to minimize environmental impacts, and possibly health hazards[1]. Therefore, power sources are desperately needed for independent, sustainable, maintenance-free, and continuous operation of such small electronics, which could be used widely for ultrasensitive chemical and biomolecular sensors, nanorobotics, micro-electromechanical systems, remote and mobile environmental sensors, homeland security, and even portable/wearable personal electronics. Therefore, new technologies that can harvest energy from the environment as *sustainable self-sufficient micro/nano-power* sources offer a possible solution. This is a newly emerging field of *nanoenergy*, which is about the applications of


ISSN:1369 7021 © Elsevier Ltd 2012

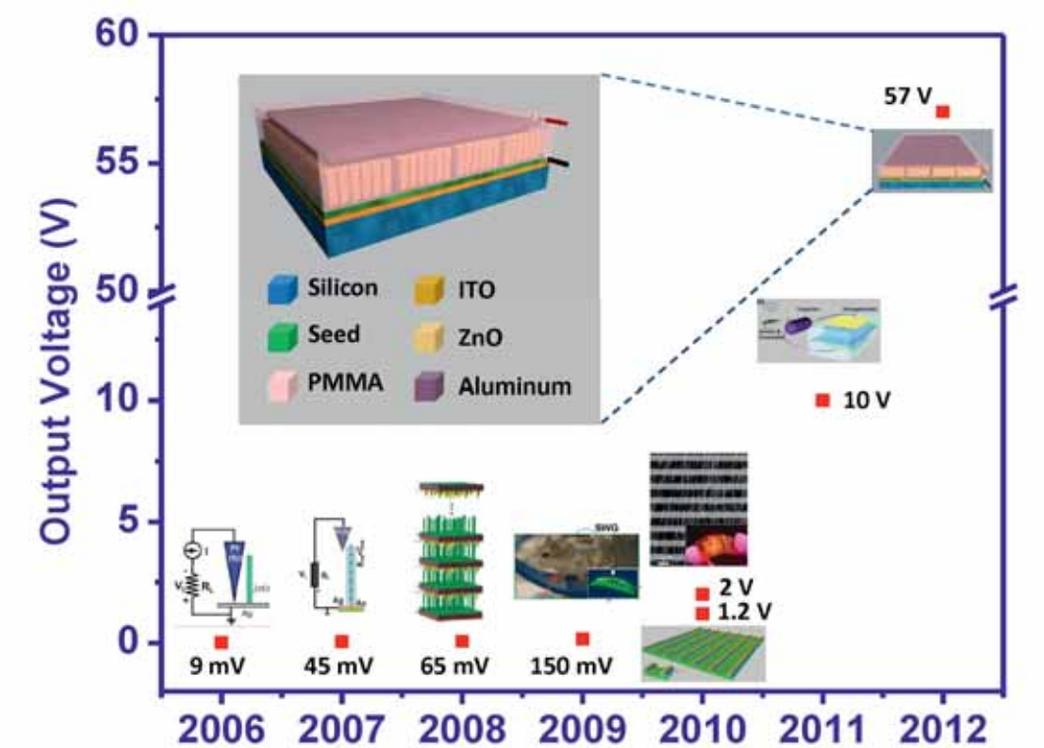


*Fig. 1 A summary on the development of high output piezoelectric nanogenerators ever since it was invented in 2006. Inset: the schematic of the mostly recently developed integrated nanogenerator based on vertically aligned ZnO arrays.*

**nanomaterials and nanotechnology for harvesting energy for powering micro/nano-systems. It can be used to possibly replace batteries or at least extend the lifetime of a battery.**

In the last 8 years, we have been developing nanogenerators (NGs) for building self-powered systems. We have mainly used three physics effects for NGs: the piezoelectric effect and triboelectric effect for harvesting mechanical energy; and the pyroelectric effect for harvesting thermal energy. A basic introduction to piezoelectric NG has been given in a recent book[2] and a few review articles[3,4]. The objective of this paper is to give a summary about the progress made in NGs in the last 3 years.

## Piezoelectric nanogenerator

The idea of a nanogenerator (NG) was first presented in 2006[5]. As an AFM tip swept across a vertically grown ZnO nanowire (NW), an electric voltage/current was generated. The working principle was attributed to the coupling between the piezoelectric and semiconducting properties of the ZnO NW. Later in 2008, a new design of NG was developed with a single ZnO NW bonded horizontally on a flexible substrate[6]. Cycled bending of the substrate produced an AC electric output from the NW. Since then, substantial progress has been made to integrate a large number of NWs together, aiming at collecting an electric current from all NWs simultaneously[7-11]. The power output has been directed along a rapidly ascending path, as shown in Fig. 1. Most recently, an integrated NG based on vertically aligned ZnO NWs was developed[12]. The peak open-circuit voltage and short-circuit current reached a record high level of 37 V and 12 μA using an NG of 1 $cm^2$ in size, respectively.

The structure of the NG is shown in the inset of Fig. 1. Vertically aligned ZnO NW arrays are sandwiched between two layers of metal electrodes. Solidified PMMA encapsulates the NWs and prevents them from intimate contact with the top metal electrode. The mechanism of the nanogenerator relies on the piezoelectric potential created in the NWs by an external strain: a dynamic straining of the NW results in a transient flow of the electrons in the external load because of the driving force of the piezopotential[8]. The advantage of using NWs is that they can be triggered by tiny physical motions and the excitation frequency can be a few Hz to multiple MHz, which is ideal for harvesting random energy in the environment such as from tiny vibrations, body motion, and gentle air flow.

The as-fabricated NG is presented in Fig. 2a. The working mechanism of the NG can be described as a transient flow of electrons driven by the piezopotential. When the NG is subject to a compressive stress, a piezopotential field is created along the NWs. As a result of the electrostatic force, inductive charges accumulate on the top and bottom electrodes[9]. In other words, the strained NWs are analogous to polarized dipole moments in a plate capacitor filled by a dielectric material. Once the stress is released, the disappearance of the piezopotential leads to a back flow of the electrons through the external circuit.

The thin layer of PMMA between the NWs and the metal electrodes is a key design that contributes to the superior performance of the newly designed NG. In our previous designs of ZnO-based NGs, Schottky contact

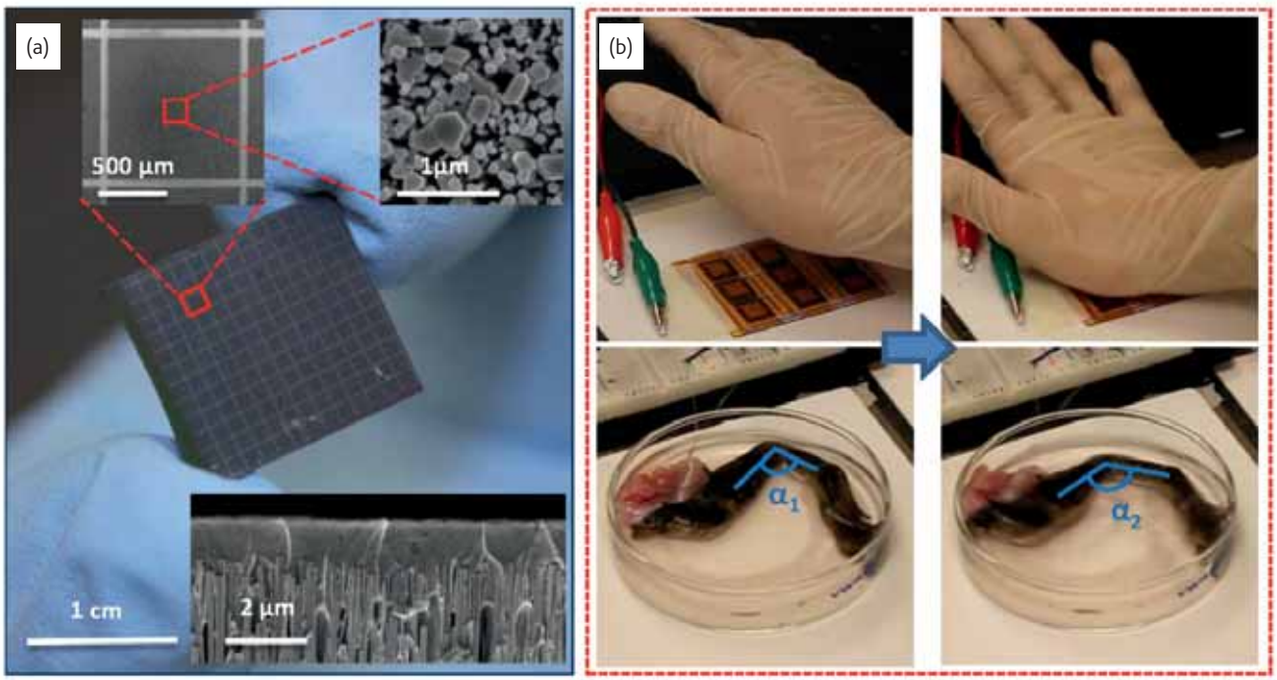


*Fig. 2 A piezoelectric nanogenerator with a maximum output open circuit voltage of 58 V and short circuit current density 12 uA/cm². (a) A picture of the as fabricated integrated NG. Insets on the top present top view of SEM images of ZnO NWs; and the inset on the bottom reveals a cross-sectional view of the NG, showing a thin layer of PMMA on top of the NWs. (b) Functional electrical stimulation of the sciatic nerve of a frog. Foot twitching is observed as a human palm impacts the NG that generates electric current pulses (with permission from the America Chemical Society).*

was required to create a potential barrier for charge accumulation[5,6]. In this work, the insulating PMMA layer provides an infinitely high potential barrier, preventing electrons from transporting through the ZnO/metal interface. Furthermore, the PMMA infiltrates into the gap between the NWs (bottom inset in Fig. 2a). As a consequence, when a compressive force is applied, the stress can be transmitted through the PMMA layer to all NWs even though they vary in length. Therefore, efficiency of the NG is greatly enhanced. In addition, it serves as a buffer layer protecting NWs from intimate mechanical interaction with the electrode, improving the NG's robustness/durability. Further, replacing PMMA by a *p*-type polymer can effectively screen *n*-type surface carriers in ZnO, resulting in an enhanced piezoelectric property and thus the electric output.

By connecting multiple NGs together in parallel into a pad (Fig. 2b), the electric power output could be further enhanced. Using the instantaneous electric output of the NG pad for each palm impact, we successfully achieved real-time functional electrical stimulation of a sciatic nerve of a frog. Note, the majority of the energy was consumed overcoming the package layer of the NGs in such a case. The NG pad was connected to an amputated hind limb of a frog by inserting the positive and negative terminals of the NG pad into the white corded sciatic nerve. A human palm impacted the NG pad to generate electric impulses. Under the instantaneous electrical input, vibrant foot twitching was observed, resulting from contraction of the gastrocnemius muscle, as visualized in Fig. 2b. The palm impact and foot twitching were perfectly synchronized, indicating real-time stimulation using the electricity generated by each impact of a palm. The output power of a NG is strong enough to drive conventional electronic components, such as an LED and a tiny liquid crystal display[10,11].

## Triboelectric nanogenerator

The triboelectric effect is a type of contact charging effect in which certain materials become electrically charged after they come into contact with other materials. According to a material's tendency to gain or lose electrons upon contact with other materials, a triboelectric series is formulated. Such an effect is usually regarded as an annoying or even hazardous phenomenon because it may lead to ignition, dust attraction, and damage to electronics. Very few efforts have been made to utilize this effect in energy harvesting. Recently, we demonstrated a miniaturized triboelectric NG with low cost and easy fabrication[13,14]. Owing to the coupling of contact charging and electrostatic induction, electric generation was achieved with repeating contact between two polymer films that differ in polarity in triboelectric series. The instantaneous electric power density reached as high as 31.2 mW/cm³.[15]

Sketched in Fig. 3a, the triboelectric generator has a multi-layer structure. Two polymer layers are separated by a spacer, forming a cavity in-between. Metal electrodes are deposited on the back of the two polymers. With an externally introduced force, the two polymers deform and contact with each other. Surface charge transfer then takes place at the contact area due to the triboelectric effect. According to the triboelectric series, electrons are injected from PMMA into Kapton, resulting in net negative charges at the Kapton surface and net positive charges at the PMMA surface. As the force is removed, the two polymers

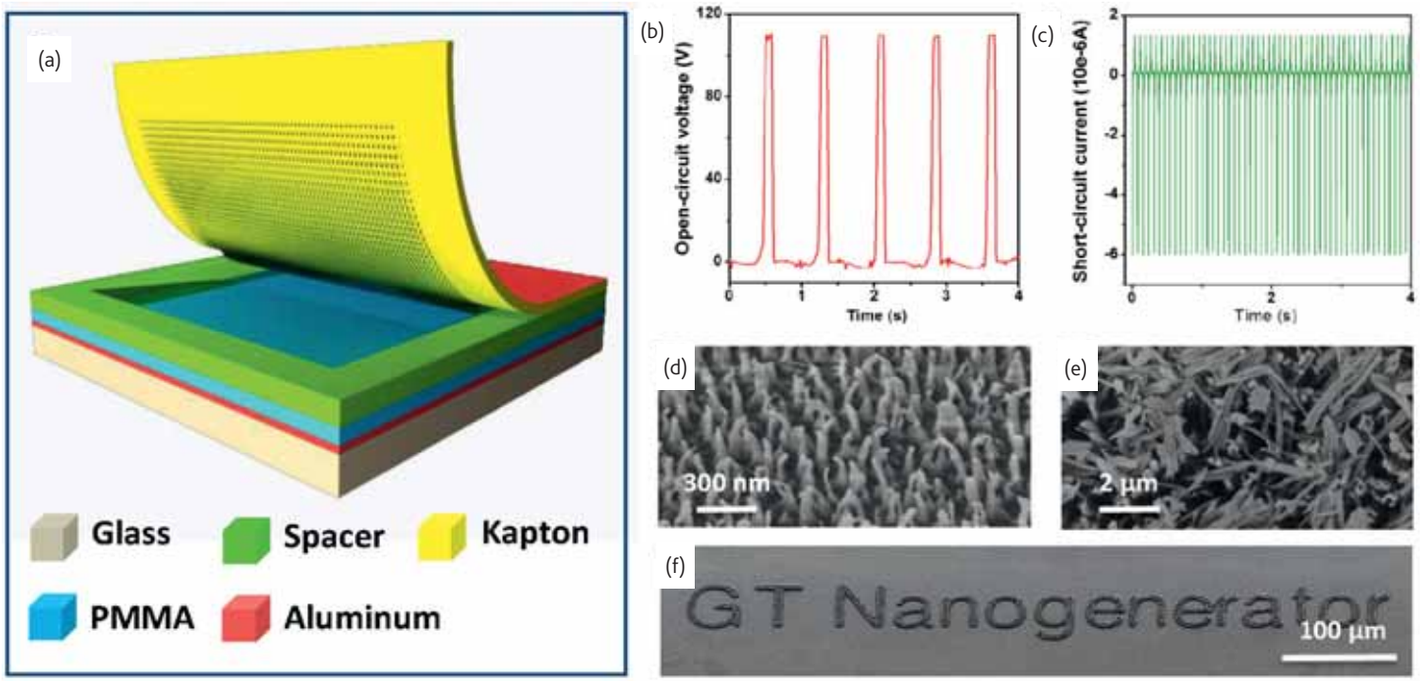


*Fig. 3 A design and performance of a triboelectric nanogenerator. (a) A schematic of the miniaturized triboelectric NG. (b) Open-circuit voltage. (c) Short-circuit current. (d) SEM image of polymer NWs on Kapton surface with proper length, showing retained orientation after 1000 times of contacts. (e) SEM image of overly long NWs that have permanent deformation after 1000 contacts. (f) Silver deposits on gold as a result of pulse electrodeposition powered by the triboelectric NG (with permission from America Chemical Society).*

separate due to the elastic properties of the polymer materials. As long as a gap forms between them, an electric potential difference is established across the two electrodes because of the separation of triboelectric charges. As a result, electrons are driven to flow through the external circuit in order to screen/eliminate such a potential difference. Based on the same reasoning, as the two polymers are brought close to each other by an external force, electrons flow back in the reverse direction.

As presented in Figs. 3b and 3c, the peak value of the open-circuit voltage and short-circuit current were up to 110 V and 6 μA for a size of 2 $cm^2$, respectively. Here, surface morphology modification was performed, creating nano-scale features to assist triboelectric charge generation. We applied selective dry etching on the Kapton surface to create vertically aligned polymer NWs. Enhanced surface roughness as a result of the NWs is expected to introduce additional friction as the two polymers are brought into contact. Such frictional movement is likely to generate more triboelectric charges; and thus enhanced electric output is achieved. However, experimental observation shows that the electric output substantially drops with excessive etching time. For NWs with a proper length (hundreds of nanometers), the elastic property ensures that the orientation and morphology of the NWs is retained, even after numerous contacts (Fig. 3d). However, NWs with a large aspect ratio are likely to be permanently deformed (Fig. 3e). Therefore, they are not able to introduce sustainable effective friction, which explains why the enhanced electric output is lower.

After rectification, the electric current from the triboelectric NG was successfully applied as a power source for pulsed electrodeposition. Micro-scale silver features, shown in Fig. 3f, were deposited on a gold substrate. This extends the application of energy-harvesting technology to the field of electrochemistry, with further utilizations including, but not limited to, pollutant degradation, corrosion protection, and water splitting. Triboelectric NG has been demonstrated to give a maximum output power on the load of 8 mW, which instantaneously drives a series of LEDs using the motion of a single finger tip, as well as outdoor sensor systems and a cell phone with the assistance of an energy storage unit[16].

## Pyroelectric nanogenerator

Pyroelectric nanogenerator is an energy harvesting device converting thermal energy into electric energy using pyroelectric effect. Usually, harvesting thermal energy mainly relies on the Seebeck effect that utilizes a temperature difference between two ends of the device for driving the diffusion of charge carriers[17]. However, when the temperature is spatially uniform without a gradient but with a time-dependent variation, the Seebeck effect cannot be used to harvest thermal energy. In this case, the pyroelectric effect has to be the choice, which is about the spontaneous polarization in certain anisotropic solids as a result of temperature fluctuation[18]. By harvesting the waste heat energy, pyroelectric nanogenerators have the potential applications such as environmental monitoring, temperature imaging, medical diagnostics, and personal electronics.

The working principle of pyroelectric nanogenerator will be explained for two different cases: the primary pyroelectric effect and the secondary

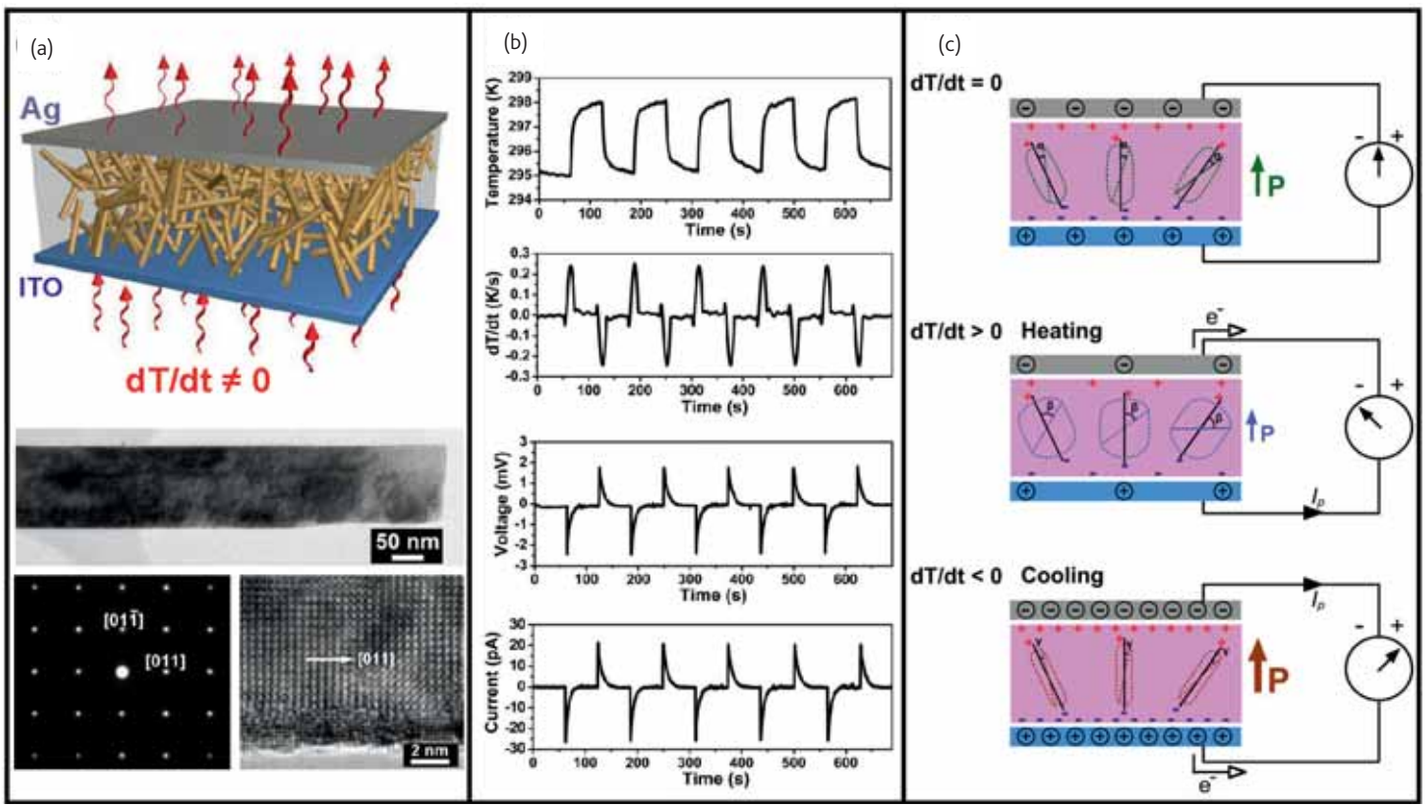


*Fig. 4 The mechanism of the pyroelectric nanogenerator based on the primary pyroelectric effect. (a) Schematic diagram of the structure of pyroelectric nanogenerator, TEM image of a single $KNbO_3$ NW, the corresponding SAED pattern of the NW, and the corresponding HRTEM image of the NW. (b) The output voltage and current of the device under the cyclic change in temperature. (c) Schematic diagrams of the pyroelectric nanogenerator with negative electric dipoles under room temperature heated and cooled conditions. The angles marked in the diagrams represent the degrees to which the dipole would oscillate as driven by statistical thermal fluctuations (with permission from Wiley).*

pyroelectric effect. The primary pyroelectric effect describes the charge produced in a strain-free case, which dominates the pyroelectric response in PZT, BTO, and some other ferroelectric materials[19-21]. The mechanism is based on the thermally induced random wobbling of the electric dipole around its equilibrium axis, the magnitude of which increases with increasing temperature[22]. Here, we used a lead-free $KNbO_3$-NW/PDMS-polymer pyroelectric composite as an example to describe it. As shown in Fig. 4a, the pyroelectric device mainly consists of three layers: an Ag film as the top electrode, a NW-composite film, and an indium tin oxide (ITO) film as the bottom electrode, where both the Ag and ITO films were used as electrodes. The diameter of the perovskite $KNbO_3$ NW is about 150 nm and the growth direction is along [011]. Fig. 4b shows the output voltage (2 mV) and current (20 pA) of the device under the cyclic change of the temperature from 295 to 298 K. The corresponding mechanism of the device is discussed in Fig. 4c. The spontaneous electric dipoles in $KNbO_3$ NWs originate from $Nb^{5+}$ ion movement in $NbO_6$ octahedra, where there are six possible orientations along the <001> directions.

Due to thermal fluctuations, the electric dipoles will randomly oscillate within a degree from the respective aligning axis. Under a fixed temperature, the total average strength of the spontaneous polarization of the electric dipoles is constant, resulting in no electric output (the top one in Fig. 4c). If we apply a change in temperature in the NG from room temperature to a higher temperature, the increase in temperature will cause the electric dipoles to oscillate with a larger range around their respective aligning axes. The total average spontaneous polarization is decreased due to the spread of the oscillation angles. The quantity of induced charges in the electrodes is thus reduced, resulting in a flow of electrons in the external circuit (the middle of Fig. 4c). If the NG is cooled instead of heated, the spontaneous polarization will be enhanced since the electric dipoles oscillate within a smaller degree of spread angles due to the lower thermal activity. The total magnitude of the polarization is increased and the amount of the induced charges in the electrodes is increased. The induced electrons will then flow in an opposite direction (the bottom of Fig. 4c).

For the second case, the pyroelectric response obtained is explained by the secondary pyroelectric effect, in which the charges are produced by the strain induced anisotropic thermal expansion. The secondary pyroelectric effect dominates the pyroelectric response in ZnO, CdS, and some other wurtzite-type materials that have a non-central symmetric structure[23]. The thermal deformation can induce a piezoelectric potential difference across the material, which can drive the electrons to flow in the external circuit. The output of the nanogenerator is associated with

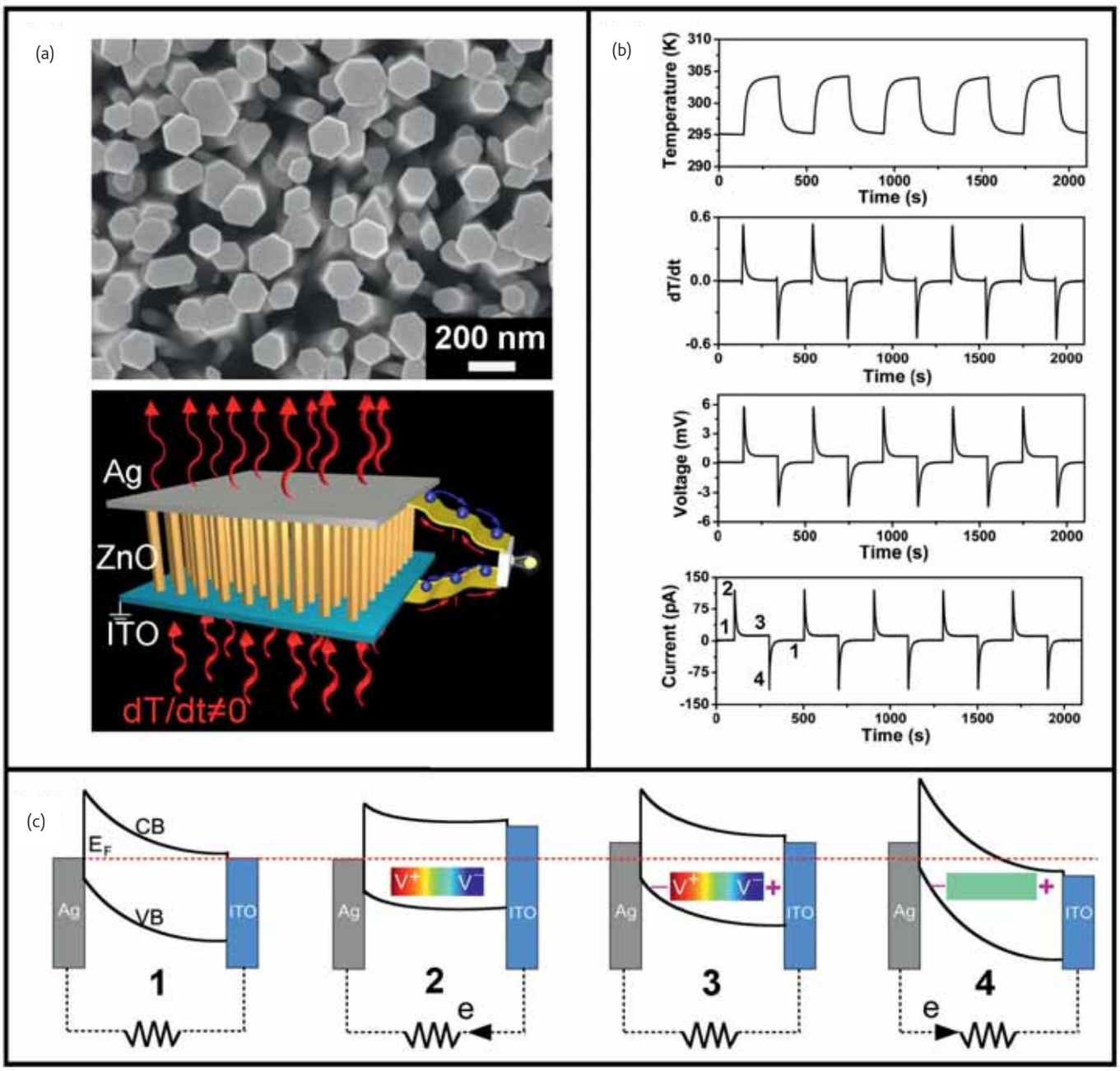


*Fig. 5 The mechanism and performance of the pyroelectric nanogenerator based on the secondary pyroelectric effect. (a) SEM image of ZnO NW array and schematic diagram of the structure of pyroelectric nanogenerator. (b) The output voltage and current of the device under the cyclic change in temperature. (c) The corresponding energy diagrams of the device at the four different stages (with permission from Wiley).*

the piezoelectric coefficient and the anisotropic thermal expansion of the material. Here, we used a ZnO NW array as an example to describe it. Fig. 5a shows an SEM image of the obtained ZnO NW array, indicating that the diameters of the NWs are about 200 nm. The schematic diagram of the device shows that it consists of an Ag film as the top electrode, ZnO NW array, and an ITO film as the bottom electrode. The corresponding output voltage (5.8 mV) and current (108.5 pA) of the device were shown in Fig. 5b, where the temperature was periodically changed from 295 to 304 K.

Fig. 5c shows the proposed mechanism for the ZnO NW array-based pyroelectric NG. The regions marked with "1-4" in Fig. 5b correspond to the numbered diagrams in Fig. 5c. When the temperature of the device was increased from 295 to 304 K, a pyroelectric electrical potential was created along ZnO NW, where the negative and positive electrical potentials are at the ITO and Ag electrodes, respectively. The conduction band and Fermi level of the ITO electrode are increased due to the negative electrical potential, driving the electrons to flow from the ITO

electrode to the Ag electrode. There was no measurable current when a new equilibrium was reached. After the temperature returned to 295 K, the accumulated electrons at the Ag electrode were released and flowed back to the ITO electrode as the pyroelectric electrical potentials disappeared.

The output current $I$ of the pyroelectric nanogenerators can be determined by the equation of $I = pA(dT/dt)$, where $p$ is the pyroelectric coefficient, $A$ is the effective area of the NG, $dT/dt$ is the rate of change in temperature[21]. Pyroelectric nanogenerators are expected to be applied in various applications where a time-dependent temperature fluctuation exists. One of the feasible applications of the pyroelectric nanogenerator is as a self-powered temperature sensor, which can work without a battery, where the response time and reset time of the sensor are about 0.9 and 3 s, respectively[24].

## Hybrid cells for concurrently harvesting multi-type energies

In our living environment, there is abundance of energy in the forms of solar, thermal, mechanical, chemical, biological, and magnetic. In order to satisfy the worldwide long-term energy needs and to achieve the sustainable and maintenance-free operation of micro/nanosystems, energy harvesting[5, 25-28] has been developed as a group of technologies to generate electricity from the ambient environment. These technologies are often based on vastly different approaches and mechanisms for different types of energy. However, all of the approaches are targeted at only one type of energy, with other types wasted. A solar cell, for example, is only designed to generate electricity under light illumination, and cannot be used at concealed locations where sunlight is not available. Since a micro/nano-system can work under variable environments and conditions, simply relying on one type of energy is insufficient to drive its operation. Thus, it is highly desirable to develop a hybrid cell (HC)[29] which can conjunctionally convert multiple types of energy into electricity, so that the energies available to us could be fully utilized and systems could be powered at any time and any place.

To fully utilize the energy in the environment, a hybrid cell was first proposed by Wang's group[30] for simultaneously harvesting multiple types of energy using a single generator (e.g., a HC that harvests both solar and mechanical energy). After this, different types of HCs[31-36] have been developed to combine the harvesting of different energy sources, such as mechanical and biochemical energy, solar and thermal energy, and mechanical and thermal energy.

### Hybrid cells for harvesting solar and mechanical energies

Photovoltaic cells or solar cells are a popular renewable energy technology, relying on approaches such as inorganic $p$-$n$ junctions, organic thin films, and organic-inorganic heterojunctions. However, a solar cell works only under sufficient light illumination, which depends on the location the devices will be deployed, as well as the time of the day and the weather. Considering that mechanical energy is widely available in our living environment, in 2009 Xu *et al.* demonstrated the first hybrid cell[30] for concurrently harvesting solar and mechanical energy through simply integrating a dye-sensitized solar cell (DSSC) and a piezoelectric nanogenerator on the two sides of a common substrate. After this, in order to solve the encapsulation problem from liquid electrolyte leakage in the first back-to-back integrated HC, early in 2011, Xu and Wang improved the prototype design of the HC and developed a compact solid state solar cell[36]. This innovative design convoluted the roles played by the NW array to simultaneously perform their functionality in a nanogenerator and a DSSC.

Based on these demonstrations of HCs for concurrently harvesting solar and mechanical energies, Pan *et at.* reported an optical fiber-based three-dimensional (3D) hybrid cell[34], consisting of a dye-sensitized solar cell for harvesting solar energy and a nanogenerator for harvesting mechanical energy; these are fabricated coaxially around a single fiber as a core–shell structure (Fig. 6a). The optical fiber, which is flexible and allows remote transmission of light, serves as the substrate for the 3D DSSC[37,38] for enhancing the electron transport property and the surface area, and making it suitable for solar power generation at remote/concealed locations. The inner layer of the HC is the DSSC portion, which is based on a radically grown ZnO NW array on an optical fiber with ITO as the bottom electrode. The dye-sensitized ZnO NW array was encapsulated by a stainless steel capillary tube with a Pt-coated inner wall as the photoanode for the DSSC. The stainless steel tube also serves as the bottom electrode for the outer layer of the nanogenerator, with densely packed ZnO NWs grown on its outer wall.

The output of the HC as voltage is presented in Fig. 6b. Due to the AC output of the NG, a current rectification was implemented using a commercial full-wave bridge rectifier in order to fully use the electrical energy harvested by the AC NG. The open-circuit voltage ($V_{OC}$) of the DSSC is about 0.4 V, and the $V_{OC}$ of the NG is about 2.9 V, resulting in a $V_{OC}$ of the HC of about 3.3 V. Fig. 6c presents the output in current from the HC under a cycled compressive strain with an average frequency of about 1 Hz. The enlarged views of the short-circuit current $I_{SC}$ of a single NG and the HC, which are marked in blue and red rectangles in Fig. 6c, are shown in Fig. 6d and e, respectively. The $I_{SC}$ of the DSSC is 7.52 μA and that of the NG is 0.13 μA; as a result, the peak $I_{SC}$ of the hybrid is 7.65 μA when the DSSC and the NG are connected in parallel with the same polarity. It can be noted that the output current of the HC is dominated by the DSSC, while the output voltage of the HC is dominated by the NG. Complementary contribution of the DSSC and NG is likely beneficial for the power output of the HC. This optical fiber-based HC shows great potential as a power source for nanosystems in the biological sciences, environmental monitoring, and even personal electronics, especially for continually powered devices at remote/concealed locations.

### Hybrid cells for harvesting biomechanical and biochemical energies

With the rapid development of *in vivo* biomedical technologies, powering implantable nanodevices for biosensing using energy harvesting technology has become an urgent requirement. Because only biomechanical, biochemical, and possibly electromagnetic energies can be harvested in the biological body, it is highly desirable to develop a technology that can scavenge biomechanical and biochemical energy simultaneously. For this purpose, Hansen *et al.* in 2010 developed a hybrid cell consisting of a piezoelectric nanofiber nanogenerator and a flexible

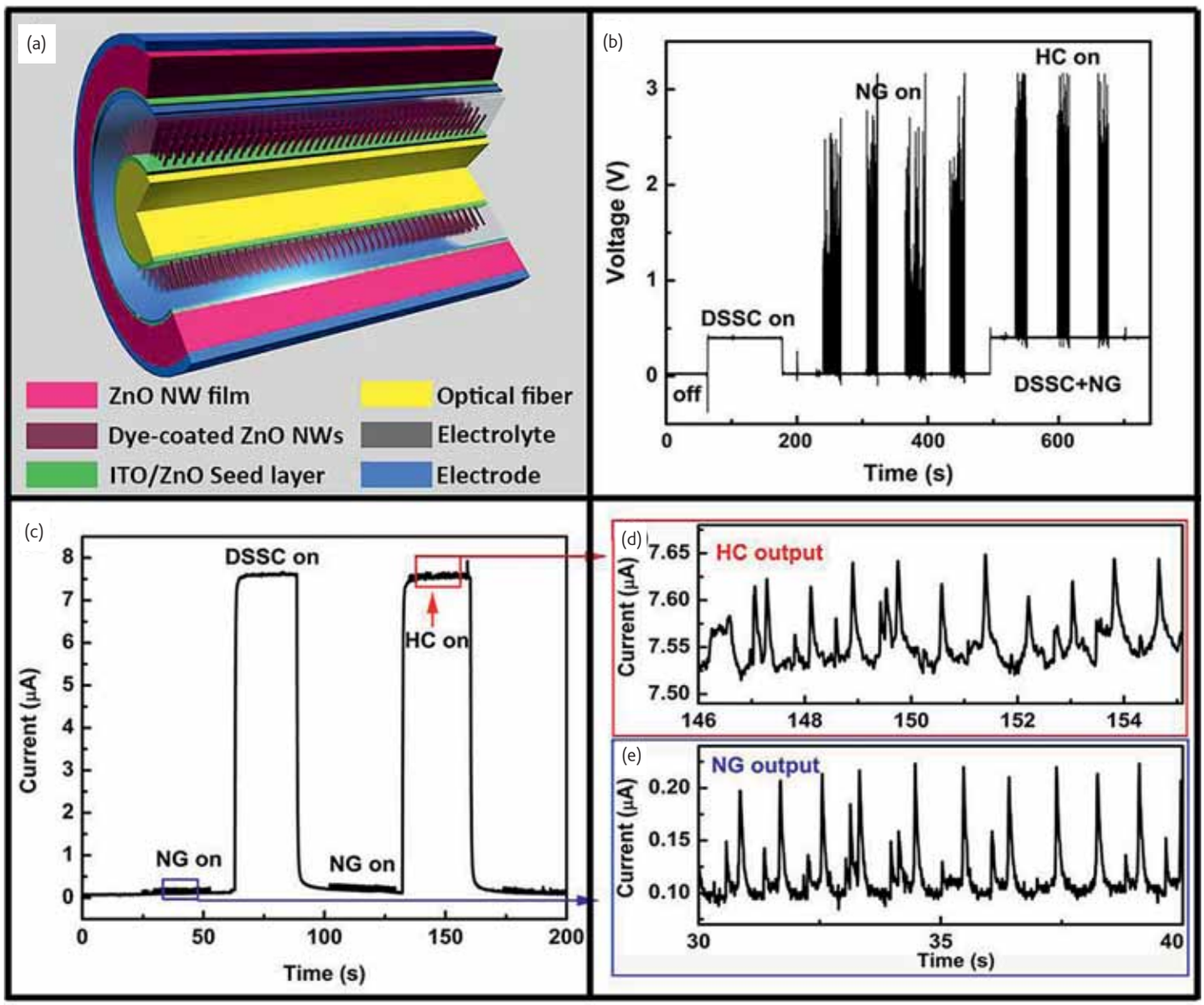


*Fig. 6. Design and performance of a 3D optical fiber based hybrid cell (HC) consisting of a dye-sensitized solar cell (DSSC) and a nanogenerator (NG) for harvesting solar and mechanical energy. (a) The 3D HC is composed of an optical fiber based DSSC with capillary tube as counter electrode and a NG on top. (b) Open-circuit voltage ($V_{OC}$) of the HC when the NG and the DSSC are connected in series, where $V_{OC(HC)}=V_{OC(DSSC)}+V_{OC(NG)}$. (c) Short-circuit current ($I_{SC}$) of the HC when the NG and the DSSC are connected in parallel. (d) and (e) Enlarged view of $I_{SC(HC)}$ and $I_{SC(NG)}$, clearly showing that $I_{SC(NG)}$ is 0.13 μA, the $I_{SC(DSSC)}$ is 7.52 μA, and the $I_{SC(HC)}$ is about 7.65 μA, nearly the sum of the output of the DSSC and the (with permission from Wiley).*

enzymatic biofuel cell separately arranged on a plastic substrate[32].

In 2011, Pan *et al*. improved the structural design and device performance[35] with a flexible fiber based HC consisting of a fiber nanogenerator (FNG) and a fiber biofuel cell (FBFC). In this fiber based HC as shown in Fig. 7a, the FNG and FBFC are integrated on a single carbon fiber for simultaneously or independently harvesting biomechanical and biochemical energies. The design of the FNG is based on the textured ZnO NW film (see the inset in Fig. 7a) grown on the surface of the carbon fiber, which serves both the bottom electrode and the substrate for ZnO growth. And the FBFC for scavenging chemical energy from a bio-fluid is fabricated at the other end of the carbon fiber.

When the HC is immersed into a bio-liquid containing glucose, the FBFC generates a DC output with a typical current of 100 nA and voltage of 100 mV. When a constant pressure is periodically applied to the bio-liquid, the FNG generates an AC output. The output voltage of the FNG achieves 3.0 V with an output current of 200 nA for an FNG consisting of ~1000 carbon fibers. By integrating the AC FNG with the DC FBFC, the HC with the output close to the sum of the FBFC and the FNG is obtained (Figs. 7b,c). The shape and frequency of the AC FNG output were the same before and after the hybridization process, with only the

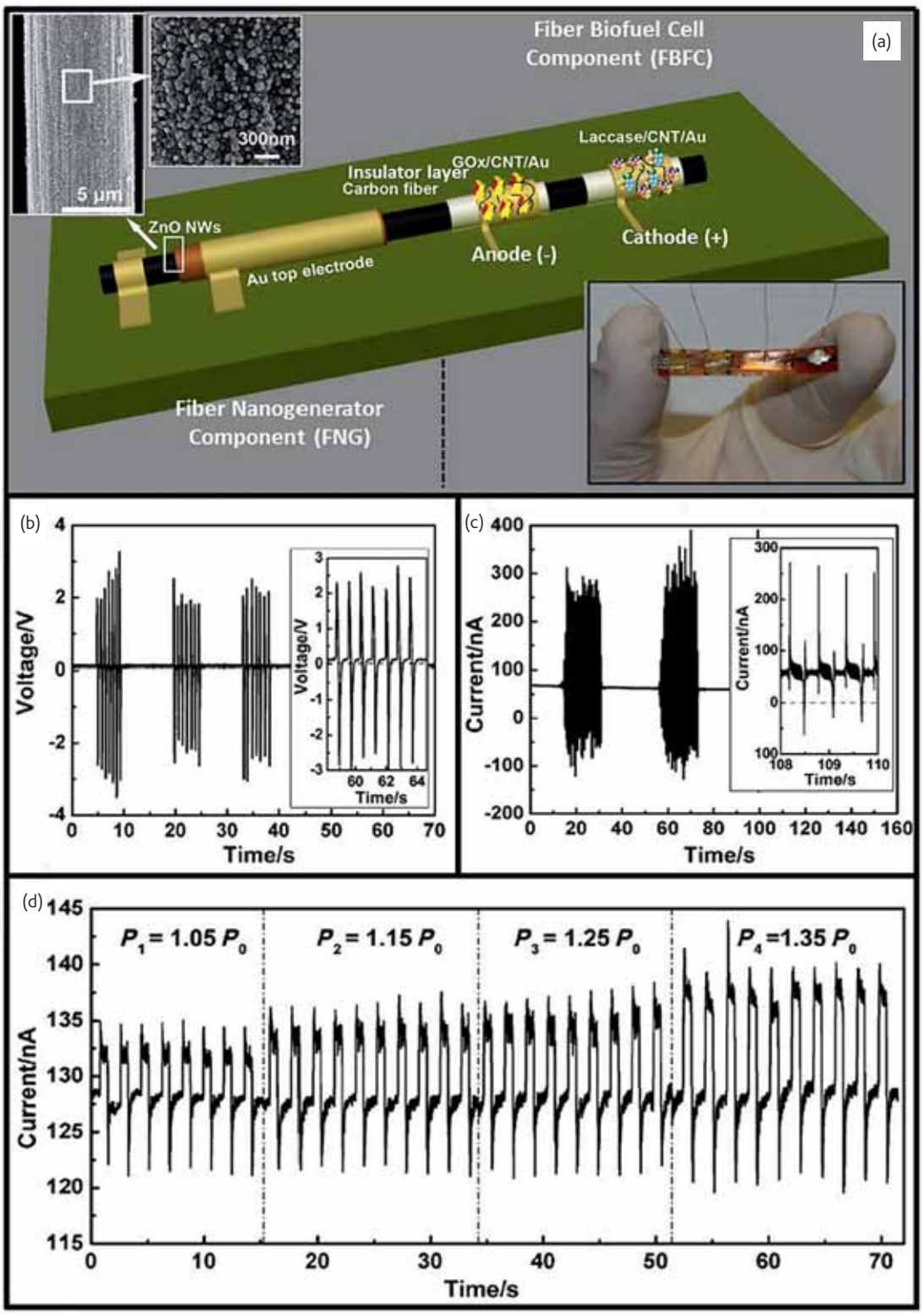


*Fig. 7 Design and electrical measurement of a single fiber-based HC for simultaneously harvesting of bichemical and biomechanical energies from an external force or pressure applied to a liquid. (a) Schematic 3D representation of the HC. The insets in the upper left are SEM images of a textured ZnO NW film grown around a carbon fiber composed of densely packed ZnO NW. A digital pircture of the device is shown at the lower corner. (b) Open-circuit voltage of the HC when the FNG and the FBFC are connected in series. (c) Short-circuit current of the HC when the FNG and the FBFC are connected in parallel. The insets in (b) and (c) are enlarged plots of the corresponding outputs showing the details of the signals; dashed lines indicated the zero-output line. (d) Response of the HC system to periodically applied pressure (with permission from Wiley).*

base line shifting from zero to the FBFC output. The peak value of the hybrid NG open-circuit voltage was ±3.1 V when they were in series; the peak values of the short-circuit current are 300 nA and –100 nA, when they were connected in parallel.

The fiber-based hybrid NG can also work as a self-powered nanosystem when FNG and FBFC are connected in series to form a loop. The FNG effectively works as a piezoelectric sensor ("load"), and the FBFC plays the role of the power source that drives the FNG, forming a self-powered system for monitoring pressure variation in a bio-liquid. We can get the magnitude of the pressure applied onto the FNG through monitoring the current in the loop. As shown in Fig. 7d, when the applied pressure increases from ambient atmosphere $P_0$ to $1.05P_0$, $1.15P_0$, $1.25P_0$, and then $1.35P_0$, the response current increases from 128 nA to 135 nA, that is, by roughly 7 %. The sensitivity of the pressure measurement demonstrated was 1.35 %. This shows the potential to monitor the pressure in a liquid, such as blood pressure in blood vessels, by monitoring the current change in the circuit.

### Hybrid cells for harvesting biomechanical and thermal energies

In some situations, a temperature fluctuation and mechanical vibration coexist, such as on human skin or near a working engine/machine. Lee *et al.*[39] have developed a hybrid cell for harvesting both thermal and mechanical energies. The thermal energy was harvested using the Seebeck effect, and the mechanical energy was harvested using piezoelectric NG. The HC is an integration of the two units, one on the top of the other, based on a flexible substrate. The output performance of the two processes can be complimentarily integrated without sacrificing the combined output, including the high output current from the thermoelectric generator and the high output voltage from the piezoelectric NG. They have demonstrated the possibility of scavenging both thermal and mechanical energies from skin temperature and body motion. This strategy provides a highly promising platform, as hybrid cells simultaneously harvest multiple types of energy such that energy resources can be effectively and complementarily utilized for power sensor networks and micro/nano-systems.

## Self-charging power cells for hybridizing energy conversion and storage

Aside from energy harvesting to generate electricity, energy storage is another equally important technology for energy science today. This technology greatly improves the flexibility of energy consumption, so that we can utilize energy to drive electronic devices/systems at any power rate and at any place. In existing technologies, energy storage is based on distinctly different mechanisms and physical systems to energy harvesting. The electrochemical-system-based units, such as Li ion batteries, are the most effective approaches to storing electricity as chemical energy through the migration of ions under the driving force of an externally applied voltage source and the resulting electrochemical reactions that occur at the anode and cathode. So in an entire energy harvesting to storage loop, the ambient energy is firstly converted into electricity, and then the electric energy is stored as chemical energy. If we can develop a hybrid cell with a fundamental mechanism that directly hybridizes the two processes into one, through which the mechanical energy is directly converted and simultaneously stored as chemical energy, it could greatly enhance the total energy conversion and storage efficiency, by avoiding the electrical energy loss on the outer circuitry in the intermediate step. This could also largely expand the application of energy harvesting and storage technology.

In order to hybridize the two distinct processes of energy conversion and energy storage into one, Wang's group in 2012 firstly developed a self-charging power cell (SCPC)[40] and introduced an unprecedented mechanism through which the mechanical energy is directly converted and simultaneously stored as chemical energy. In this manner, the nanogenerator and the battery are hybridized as a single unit. The SCPC is realized by replacing the polyethylene (PE) separator used in conventional Li batteries with a piezoelectric poly(vinylidene fluoride) (PVDF) film (Fig. 8a), which integrates the characteristics of both a piezoelectric and the electrochemical properties. The device is based on a sealed stainless-steel 2016-coin-type cell filled with an electrolyte, as shown in the highlight of Fig. 8b. The SCPC is composed of three major components: anode, separator, and cathode. The anode layer consists of an aligned $TiO_2$ nanotube array grown directly on a Ti foil. Instead of using the polyethylene (PE) separator[41] as in a traditional lithium ion battery, a layer of polarized poly(vinylidene fluoride) (PVDF) film serves as the separator. This PVDF film can establish a piezoelectric potential across its thickness under externally applied stress, which not only converts mechanical energy into electricity, but also serves as the driving force for the migration of Li ions. The cathodes are $LiCoO_2$/conductive carbon/binder mixtures on aluminum foils.

The working mechanism of the self-charging power cell is an electrochemical process driven by deformation created piezoelectric potential. At the very beginning, the device is at a discharged state, with $LiCoO_2$ as the positive electrode (cathode) material and $TiO_2$ NTs as the negative electrode (anode), which is the originally fabricated structure of the device, and the $LiPF_6$ electrolyte is evenly distributed across the entire space, as shown in Fig. 8c. When a compressive stress is applied onto the device, the PVDF film will establish a piezoelectric field with a direction from the cathode to the anode (Fig. 8d). This piezoelectric field will drive Li ions in the electrolyte to migrate along the direction through the ionic conduction paths present in the PVDF film separator for ion conduction in order to screen the piezoelectric field, and finally reach the anode. The decreased concentration of $Li^+$ at the cathode will break the chemical equilibrium of the cathode electrode reaction ($LiCoO_2 \leftrightarrow Li_{1-x}CoO_2 + xLi^+ + xe^-$), so that $Li^+$ will deintercalate from $LiCoO_2$, turning it into $Li_{1-x}CoO_2$ and leaving free electrons at the current collector (Al foil) of the cathode electrode. In the meanwhile, under the elevated concentration of $Li^+$ at the anode, the reaction at the other electrode ($TiO_2 + xLi^+ + xe^- \leftrightarrow Li_xO_2$) will move to the forward direction for the same reason, enabling $Li^+$ to react with $TiO_2$ so that $Li_xTiO_2$ will be produced at the anode electrode, leaving the positive charges at the Ti foil as the current collector. During this process, $Li^+$ will continuously migrate from the cathode to the anode and the device is charged up a little bit owing to the large volume of the device. During the progress of charging electrochemical reactions at the two electrodes, extra free electrons will transfer from the cathode to the anode, in order to maintain the charge neutrality and the continuity of the

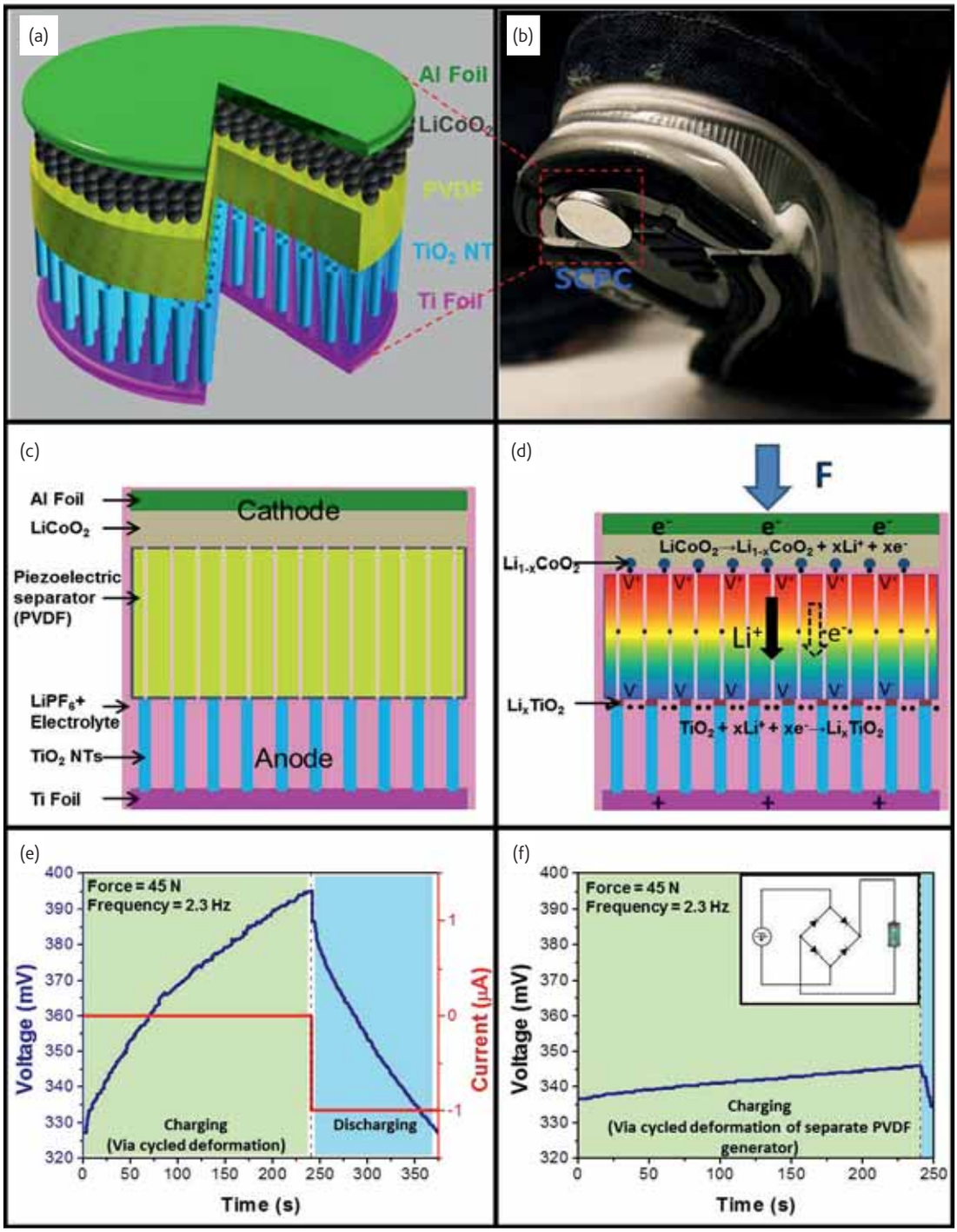


*Fig. 8 A self-charging power cell (SCPC) that hybridizes a piezoelectric nanogenerator and a Li-ion battery. (a) Schematic diagram showing the design and structure of the SCPC. The anode is aligned $TiO_2$ nanotube arrays that are directly grown on Ti foils; a layer of polarized PVDF film performs as the separator; the cathode is $LiCoO_2$ mixture on aluminum foil. (b) Sticking a power cell on the bottom of a shoe, the compressive energy generated by walking can be converted and stored directly by SCPC. (c) & (d) The brief working mechanism of the SCPC driven by compressive straining: (c) schematic illustration of the SCPC in discharged state with $LiCoO_2$ as cathode and $TiO_2$ nanotubes as anode; (d) under the driving of the piezoelectric field from straining, the Li ions from the cathode will migrate through the PVDF film separator in the electrolyte toward the anode, leading to the corresponding charging reactions at the two electrodes. The free electrons at the cathode and positive charges at the anode will dissipate inside the device system. (e) A typical self-charging process simply by applying cycled mechanical compressive strain to the device (green shadowed region), during which the voltage keeps raising; in the discharge process (blue shadowed region), the stored power is released in the form of electron flow in the external load. (f) As a comparison of efficiency, the SCPC is separated into two individual units: a PVDF piezoelectric generator and a Li-ion battery by using PE as a separator. The inset is a schematic circuit of the traditional charging methods with separated generator and storage units connected by a bridge rectifier (with permission from the America Chemical Society).*

charging reaction. There should probably be some internal mechanisms for the electrons to transfer across the two electrodes, although this exact process is still to be further investigated. This is the process of converting mechanical energy directly into chemical energy.

By using a mechanical setup that can provide a periodic compressive stress onto the device, the self-charging process of the power cell was demonstrated. Fig. 8e is a typical self-charging and discharging cycle. Under the compressive force applied to the SCPC at a frequency of 2.3 Hz, the voltage of the device increased from 327 to 395 mV in 240 s. After the self-charging process, the device was discharged back to its original voltage of 327 mV under a discharge current of 1 μA, which lasted for about 130 s. The stored electric capacity of the power cell was about 0.036 μAh. We compared the SCPC with the traditional charging method, which is composed of a separated generator and a storage unit connected though a bridge rectifier (inset of Fig. 8f). The generator unit was fabricated by sealing the PVDF film in the same coin cell to create a similar straining condition as SCPC. After being charged for 4 min via cycled deformation of the separate PVDF generator, the voltage of the battery only increased by ~10 mV (Fig. 8f), which is a lot lower than that of SCPC (65 mV). Therefore, the single mechanical to chemical process for SCPC is much more efficient than the mechanical to electric and then electrical to chemical double-processes for charging a traditional battery. This is because of the new approach for directly converting mechanical energy into chemical energy without going through the generation of electricity as an intermediate state, that the system demonstrates, which saves at least the energy wasted on the outer circuitry, including the rectifying component. This is the innovation of the power cell.

## Summary

As first reported in 2006, nanogenerators have been an active area of research. Starting from the fundamental proof of concept, we have developed various approaches for harvesting mechanical energy and thermal energy based on piezoelectric and pyroelectric effects, respectively. By using the energy from our living environment, our goal is to make self-powered systems that can operate wirelessly, independently, and sustainably. We have demonstrated various applications of using the NG technology for powering various mobile electronics. We have also developed various hybrid cell technologies for simultaneously harvesting multiple types of energy so that we can use all of the available energy in the environment where the devices are being deployed. Lastly, integrated self-charging power cells provide an innovative approach for hybridizing a nanogenerator with an energy storage unit, as a convoluted system. The nanogenerator technology will soon impact our lives!

Besides targeting worldwide energy needs, at a large scale, we aim to address the energy required for sustainable and maintenance free operation of micro/nano-systems and mobile/portable electronics. This is the area of *nanoenergy*. The self-powering approaches developed here are a new paradigm in nanotechnology for truly achieving sustainable self-sufficient micro/nano-systems, which are of critical importance for sensing, medical science, infrastructure/environmental monitoring, defense technology, and even personal electronics.

Acknowledgements. Research was supported by DARPA, BES DOE, NSF, Airforce, Samsung and MANA NIMS (Japan). We thank Wenxi Guo, Dr. Zetang Li, Dr. Lin Dong, Dr. Xinyu Xue, Dr. Youfan Hu, Fengru Fan, Yusheng Zhou, Long Lin, Ying Liu, Dr. Yan Zhang, Aurelia C. Wang, Ruomeng Yu, Dr. Jong Hoon Jung, Chih-Yen Chen, Ken C. Pradel and Dr. Jyh-Ming Wu for their contributions to the work reviewed here. mt

## References


1. Wang, Z.L., *Adv. Mater.*, (2011) **24**, 280.
2. Wang, Z.L., *Nanogenerators for Self-Powered Devices and Systems*, published by Georgia Institute of Technology: http://smartech.gatech.edu/handle/1853/39262
3. Wang, Z.L., *Mater Sciand Engi Reports* (2009) **64**, 33
4. Wang, Z.L., *et al.*, *Mater Sci and Eng Reports* (2010) **R70**, 320.
5. Wang, Z. L., *et al.*, *Science* (2006) **312**, 242
6. Yang, R. S., *et al.*, *Nature Nanotech* (2009) **4**, 34
7. Xu, S., *et al.*, *Nano Lett* (2008) **8**, 4027
8. Yang, R. S., *et al.*, *Nano Lett* (2009) **9**, 1201
9. Xu, S., *et al.*, *Nature Nanotech* (2010) **5**, 366
10. Zhu, G., *et al.*, *Nano Lett* (2010) **10**, 3151
11. Hu, Y., *et al.*, *Nano Lett* (2011) **11**, 2572
12. Zhu, G., *et al.*, *Nano Lett* (2012) **12**, 3086
13. Fan, F.R., et al, *Nano Energy* (2012) **1**, 328.
14. Fan, F.R. *et al.*, *Nano Letters* (2012) **12**, 3109
15. Zhu, G., *et al.*, *Nano Lett* (2012) **12**, 4960
16. Wang, S.H., *et al.*, *Nano Lett* (2012) **12**, 6339.
17. Heremans, J. P., *et al.*, *Science* (2008) **321**, 554.
18. Olsen, R. B., and Evans, D., *J Appl Phys* (1983) **54**, 5941.
19. Ehre, D., *et al.*, *Science* (2010) **327**, 672.
20. Zook, J. D., *et al.*, *J Appl Phys* (1978) **49**, 4604.
21. Ye, C., *et al.*, *J Appl Phys* (1991) **70**, 5538.
22. Yang, Y., *et al.*, *Adv Mater* (2012) **24**, 5357.
23. Yang, Y., *et al.*, *Nano Lett* (2012) **12**, 2833.
24. Yang, Y., *et al.*, *ACS Nano* (2012) **6**, 8456.
25. Dresselhaus, M. S., and Thomas, I. L., *Nature* (2001) **414**, 332.
26. Oregan, B., and Gratzel, M., *Nature* (1991) **353**, 737.
27. DiSalvo, F. J., *Science* (1999) **285**, 703.
28. Poudel, B., *et al.*, *Science* (2008) **320**, 634.
29. Xu, C., *et al.*, *Nano Energy* (2012) **1**, 259.
30. Xu, C., *et al.*, *J Am Chem Soc* (2009) **131**, 5866.
31. Guo, X. Z., *et al.*, *J Power Sources* (2010) **195**, 7684.
32. Hansen, B. J., *et al.*, *ACS Nano* (2010) **4**, 3647.
33. Lee, M., *et al.*, *J Phys Chem Lett* (2010) **1**, 2929.
34. Pan, C. F., *et al.*, *Adv Mater* (2012) **24**, 3356.
35. Pan, C. F., *et al.*, *Angew Chem Int Edit* (2011) **50**, 11192.
36. Xu, C., and Wang, Z. L., *Adv Mater* (2011) **23**, 873.
37. Weintraub, B., *et al.*, *Angew Chem Int Edit* (2009) **48**, 8981.
38. Guo, W. X., *et al.*, *Nano Energy* (2012) **1**, 176.
39. Lee, S.M., *et al.*, submitted.
40. Xue, X. Y., *et al.*, *Nano Lett* (2012) **12**, 5048.
41. Zhang, S. S., *J Power Sources* (2007) **164**, 351.